 doi:10.20944/preprints202206.0151.v1

Research on forecast and suppression splashing method of AOD furnace

Changjun Guan*
School of Electrical and Electronic Engineering, Changchun University of Technology, Changchun130012, China
* Corresponding author: E-mail: guanchangjun@ccut.edu.cn

ABSTRACT: During the smelting process of AOD furnace, the unbalanced reaction of material will lead to the occurrence of splashing. It will not only damage the smelting equipment, but also seriously injure the personnel. In this study, first, the information of liquid level, audio information, and vibration information are detected by multiple sensors respectively. Then, the fused information is used to forecast the splashing. Finally, the multitasking fuzzy controller is used to suppress splashing. The results show that the method of forecasting and suppressing splashing can accurately forecast and achieve rapid suppression. Thus, the efficiency of smelting can be improved.

KEYWORDS: Forecast splashing; suppression splashing; AOD; signal fusion; fuzzy control

1. Introduction

The Argon Oxygen Decarburization (AOD) process is mixed with argon inert gases and injected through submerged tuyeres. At the gas-liquid interface, the oxygen molecule reacts with the C atom in an oxidation reaction, and the resulting CO gas escapes with the argon gas rising [1]. If the escaping gas is blocked by the excessively foamed slag, the slag and melt overflow the furnace mouth. It's called splashing. When splashing occurs, the lesser result is longer smelting time, increased gas supply and additive consumption, and the more serious consequence is that a large amount of metal splash or even damage the equipment. A severe splashing accident is shown in Figure 1. Therefore, forecasting and suppression splashing technology is one of the key technologies involved in production safety and energy saving in AOD process.

Figure 1. Severe splashing accident

For a long time, many smelting plants and research institutes have done a lot of research and practical work on prevention splashing based on the mechanism of

 doi:10.20944/preprints202206.0151.v1

splashing occurrence [2]. Common forecasting splashing methods include: sound intensity forecasting method, vibration forecasting method, furnace mouth light intensity forecasting method and furnace gas analysis forecasting method. It was found that the accuracy of audio prediction could reach 89% and the accuracy of furnace vibration frequency prediction could reach 81% [3], while the accuracy of image prediction by environmental interference could reach only 85% [4-6]. Although prediction splashing research has achieved some success, false predictions often occur when splashing is predicted by a single characteristic signal under the influence of a complex high-temperature smelting environment and multiple interference signals. In order to improve the prediction accuracy, this work proposes a forecasting method based on multi-information weighted fusion and a suppression splashing method based on multi-object fuzzy control.

2. Detecting and fusing the splashing signals

Various phenomena such as the increase in liquid level, change in furnace vibration frequency, and change in audio at the furnace mouth represent changes in the smelting state [7,8]. Therefore, this study extracts multiple information characterizing splashing by effective detection means and signal processing techniques. Multiple signals for predicting splashing are fused into one signal. The accuracy of multiple information fusion is higher than that of individual information in predicting the accuracy of splashing.

2.1 Signal detection

1) Liquid level signal detection

Complex redox reactions occur during smelting [9]. When the slags contain too much FeO and Cr_2O_3, the slags are more viscous and the venting property becomes worse. A foam splashing accident occurs when the liquid level exceeds the furnace opening height. When splashing occurs, the rise of the melt pool level is an observable phenomenon, so it can be used as one of the information for forecasting splashing accidents. The method of contact detection of melt pool level is difficult to achieve due to the extremely harsh environment of high-temperature smelting. Therefore, non-contact time-difference gas-mediated ultrasonic level sensors are used to detect the level of the melt pool. The liquid level height is determined by the variation of the distance between the emission point and the liquid level measured by the sensor [10], as shown in Equation (1).

$$h = H - L = H - \frac{v \times t}{2} \quad (1)$$

Where, H is the distance from the ultrasonic probe to the bottom of the argon-oxygen refining furnace, L is the distance from the ultrasonic probe to the liquid surface, v is the propagation speed of ultrasonic waves in the flue gas medium, t is the time consumed for ultrasonic waves to be sent and received, and h is the height of the liquid surface.

The principle of liquid level measurement by ultrasonic sensors is shown in Figure 2.

Preprints (www.preprints.org) | NOT PEER-REVIEWED | Posted: 10 June 2022 doi:10.20944/preprints202206.0151.v1

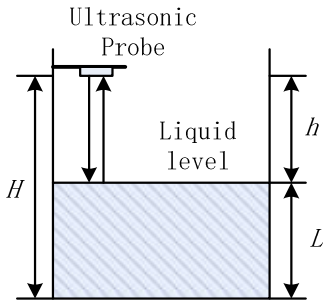

Figure 2. Principle diagram of ultrasonic level measurement

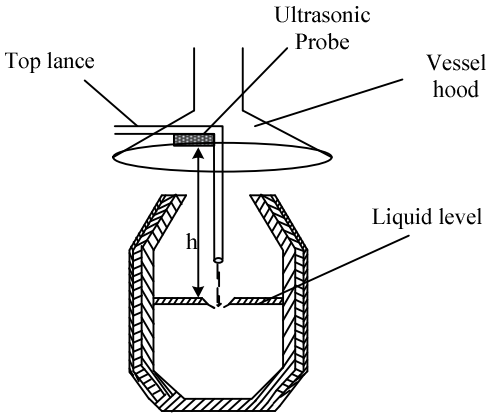

Figure 3. Schematic diagram of detecting liquid level

An ultrasonic distance measuring device is installed on the fume hood to detect the liquid level in the melt pool in real time, and the liquid level information is transmitted to the controller as one of the information for forecasting splashing. The detection principle is shown in Figure 3.

2) Detection of audio signals

Vibrational energy propagates through the medium (solid, liquid or gas) in the form of mechanical waves of pressure and displacement. Acoustic waves are generated when the medium alternately expands and compresses at a certain frequency [11]. The conduction velocity of acoustic waves is influenced by the density and pressure of the medium. And the medium density is determined by the medium temperature, state of motion and viscosity. During argon-oxygen refining of ferrochrome alloys, the gas is mixed with the melt. The medium changes before the splashing occurs. The mixing of different media affects the speed of sound and vibration frequency [12]. In addition, the stress at volumetric strain of these bubbles is relieved, which reduces the bulk modulus. However, the average density of the medium does not change significantly [13]. This is the principle of using audio signals to predict splashing.

The propagation rate of an acoustic wave in the direction perpendicular to the unit surface area is the audio intensity. For a one-dimensional plane wave, the audio intensity I is calculated by equation (2).

$$I = \frac{F^2}{\rho v} \qquad (2)$$

Preprints (www.preprints.org) | NOT PEER-REVIEWED | Posted: 10 June 2022 doi:10.20944/preprints202206.0151.v1

Where F is the pressure in N, v is the velocity in m/s, and ρ is the density of the melt.

Integrating the intensity over the surface area of the sound source yields the sound power per unit area [14], as shown in Equation (3).

$$P = \int_S IdS \tag{3}$$

When the liquid is mixed with bubbles, the volume fluctuations of the bubbles exert high acoustic pressure on the medium. Volume fluctuations cause the bubble wall to vibrate [15]. Bubbles rising along an irregular path can produce continuous low-frequency sound waves [16]. The size and number of bubbles increase with the smelting process, and the amplitude of the sound waves gradually increases. A free-field type super directional microphone is used to detect the audio signal from the melt pool and is used to forecast splashing. The physical audio signal detection system is shown in Figure 4.

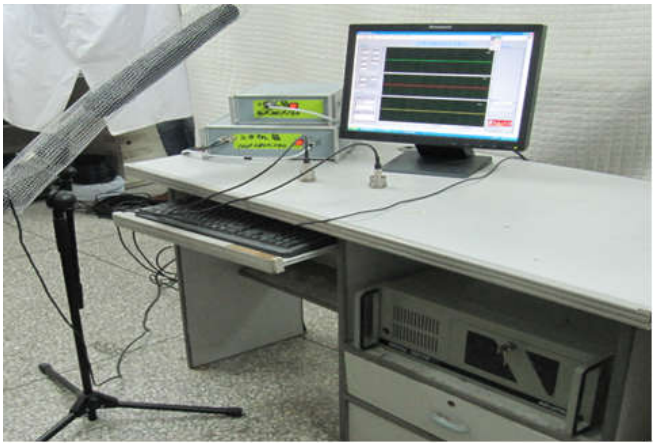

Figure 4. Audio signal detection and processing system physical

3) Detection the vibration frequency of the furnace body

According to the vibration theory, the body of argon-oxygen refining furnace will produce a certain vibration frequency under the action of periodic excitation force of melt. The melt vibration frequency is shown in the following equation.

$$\omega = \sqrt{\frac{1.84g}{r} th\left(\frac{1.84H}{r}\right)} \tag{5}$$

$$f = \frac{\omega}{2\pi} = \frac{1}{2\pi}\sqrt{\frac{1.84g}{r} th\left(\frac{1.84H}{r}\right)} \tag{6}$$

Where H is the melt height in m, g is the acceleration of gravity, r is the melt pool radius in m, and t is the time in s.

The trunnion is tightly connected to the furnace body. The low-frequency vibration signal detected by the vibration sensor on the trunnion characterizes the melt pool fluctuations. It is used to forecast splashing [17]. The sensor is mounted as shown in Figure 5.

Preprints (www.preprints.org) | NOT PEER-REVIEWED | Posted: 10 June 2022 doi:10.20944/preprints202206.0151.v1

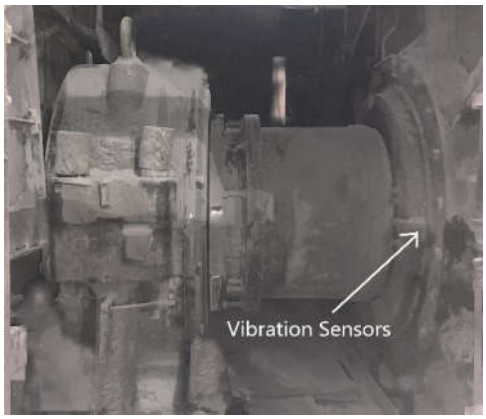

Figure 5. Schematic diagram of vibration sensor installation

2.2 Characterization signal fusion

In this work, a weighted fusion algorithm of level information, audio information and vibration information are proposed to forecast splashing accidents in argon-oxygen refining of ferrochrome alloys. First, the information of different splashing representations is normalized. Then, the signals for predicting splashing degree are obtained by weighting the fusion based on the forecast accuracy of each information.

The structure of the weighted fusion algorithm is shown in Figure 6.

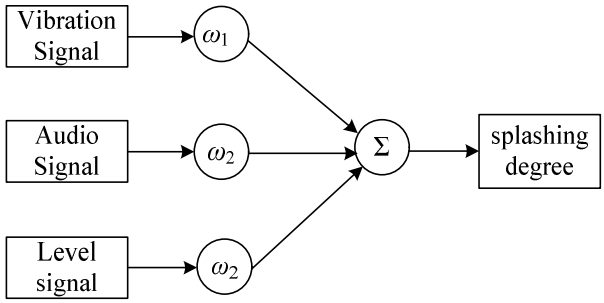

Figure 6. Weighted fusion algorithm structure diagram

First, weights are calculated based on the forecast accuracy of each of the three types of information. Then, the data processed vibration frequency signal, furnace audio signal and liquid level signal are normalized and calculated to form a value between (0,1). It characterizes the degree of splashing. In this study, the optimized variance is used to fuse the signals. Let the optimized measurement variance of the three sensors be σ_1, σ_2, and σ_3, the detection values at a certain moment be x_1, x_2, and x_3, the optimal weights be ω_1, ω_2, and ω_3, and the fusion value be $\hat{x}$. The adaptive weighting algorithm is as follows.

$$\begin{cases} \sum_{i=1}^{n} \omega_i = 1 \\ \sigma^2 = \sum_{i=1}^{n} {\omega_i}^2 {\sigma_i}^2 \end{cases} \quad (7)$$

where σ^2 is the mean squared deviation.

The extreme value theorem for multivariate functions is calculated as follows.

Preprints (www.preprints.org) | NOT PEER-REVIEWED | Posted: 10 June 2022 doi:10.20944/preprints202206.0151.v1

$$\begin{cases} \omega_i = \frac{1}{\sigma_i{}^2 \sum_{i=1}^{n} \frac{1}{\sigma_i{}^2}} \\ \sigma_{min}{}^2 = \sum_{i=1}^{n} \frac{1}{\sigma_i{}^2} \end{cases} \quad (8)$$

Equation (8) is substituted into Equation (7) to obtain the weighted fusion signal as follows.

$$\hat{x} = \sum_{i=1}^{n} x_i \omega_i \quad (9)$$

3. Suppression splashing system based on multi-object fuzzy control

The AOD furnace suppression splashing system is characterized by the coupling of multiple controlled quantities and inaccurate models, so that accurate models cannot be obtained. Fuzzy control is suitable for systems with multiple variables and imprecise models. In this work, a multi-object fuzzy control algorithm for suppression splashing was designed. The forecast signal is used as input to the fuzzy controller, and the output quantities are the top gun height, top gun gas supply control, slag composition adjuster input, bottom gun oxygen supply flow and bottom gun argon supply flow.

3.1 Fuzzy control rules

At the beginning of refining, the slags thickness is thin. As the redox reaction process intensifies, the slags accumulate and expand, forming foam slags. The foam slags can absorb noise and vibration. The relationship between noise frequency and vibration frequency of AOD furnace smelting process and the degree of slag frothing is as follows: the degree of slag frothing gradually, the slag layer thickens, the audio coming from the furnace mouth decreases, and the degree of furnace vibration weakens. The thicker the slag layer the weaker the venting properties. The possibility of frothy splashing is increasing. From the above analysis, the values of the splashing characterization signal are classified into different degrees of splashing. In the (0,1) interval, the splashing degree was divided into four segments, namely (0,0.25], (0.25,0.5] , (0.5,0.75) and [0.75,1). The degree of splashing corresponds to the control rule sets R_1 to R_4, respectively. the form of the inference statement is as follows.

If $P \in (0,0.25]$ then R_1;
If $P \in (0.25,0.5]$ then R_2;
If $P \in (0.5,0.75)$then R_3;
If $P \in [0.75,1)$then R_4.

Based on the principles of the smelting process and the experience of the technicians, the control rules are set as follows.

When the signal strength belongs to (0,0.25], the splashing is suppressed according to the R_1 rule. Specific operations are as follows: the height of the top gun is adjusted higher from 1.4m to 1.5m, the oxygen supply to the top gun is reduced by 5%-10%, and the oxygen supply and argon supply to the bottom gun are reduced by 5%-10%, thus lowering the temperature of the melt pool and reducing the gas escaping from the furnace. The feeding system puts 0-0.5t inhibitor into the molten pool to reduce the content of FeO and Cr_3O_2 in the slag, adjust the slag viscosity and increase the slag venting capacity. Splashing is prevented by these operations.

When the signal strength belongs to $(0.25,0.5]$, the splashing is suppressed

Preprints (www.preprints.org) | NOT PEER-REVIEWED | Posted: 10 June 2022 doi:10.20944/preprints202206.0151.v1

according to the R_2 rule. Specific operation is as follows: the height of the top gun is adjusted from 1.4m to 1.7m, the oxygen supply flow of the top gun is reduced by 10%-20%, and the oxygen supply and argon supply flow of the bottom gun are reduced by 10%-20%. Feeding system put 0.5-1t inhibitor into the melt pool.

When the signal strength belongs to $(0.5,0.75]$, the sputtering is suppressed according to the R_3 rule. Specific operation is as follows: Stop top gun blowing gas. Feeding system puts 1.0-1.5t of foam slag inhibitor into the melt pool. Reduce the oxygen supply and argon supply to the bottom gun by 10%-30%. Lower the melt pool temperature and reduce the gas escaping from the furnace.

When the signal strength belongs to $(0.75,1)$, the sputtering is suppressed according to the R_4 rule. Specific operation is as follows: In order to cool down quickly, the top gun height is reduced to 1.1m and switched to argon supply. The feed system puts 1.5-2t of foam slag inhibitor into the melt pool. The bottom gun stops oxygen supply and supplies argon at the minimum rate

Splashing is quickly suppressed by the above operation. The structure of the suppression splashing system is shown in Figure 7.

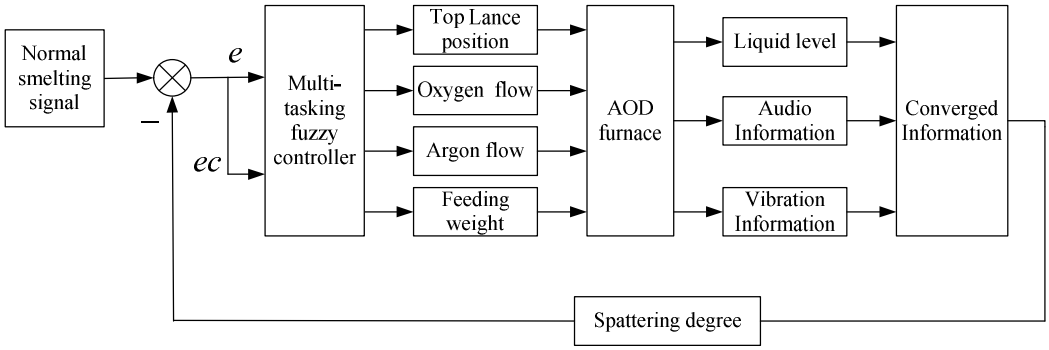

Figure 7. Multi-object fuzzy suppression splashing system structure diagram

3.2 Multi-object fuzzy controller

1) Affiliation function

The input linguistic variables for the multiobject fuzzy control designed in this study are the splashing degree deviation e and its rate of change ec. The output linguistic variables are the top gun height U, the oxygen supply flow Q_O, the argon supply flow Q_{Ar}, and the splashing inhibitor input W.

Set the fuzzy domain of the output variables as {-2, -1,0,1,2}.

The deviation $e_1 \in (-0.25,0]$ when the splashing degree signal falls into the (0,0.25] interval. e_1 is $\{e_{11},e_{12},e_{13},e_{14}\}$ and ec is $\{N,Z,P\}$.

The deviation $e_2 \in (-0.5,-0.25]$ when the splashing degree signal falls into the (0.25,0.5] interval. e_2 is $\{e_{21},e_{22},e_{23},e_{24}\}$ and ec is $\{N,Z,P\}$.

The deviation $e_3 \in (-0.75,-0.5]$ when the splashing degree signal falls into the (0.5,0.75] interval. e_3 is $\{e_{31},e_{32},e_{33},e_{34}\}$ and ec is $\{N,Z,P\}$.

The deviation $e_4 \in (-1,-0.75]$ when the splashing degree signal falls into the (0.75,1) interval. e_4 is $\{e_{41},e_{42},e_{43},e_{44}\}$and ec is $\{N,Z,P\}$.

The fuzzy set of U is { *PU1,PU2,PU3,PU4* }.

Preprints (www.preprints.org) | NOT PEER-REVIEWED | Posted: 10 June 2022 doi:10.20944/preprints202206.0151.v1

The fuzzy set of Q_O is {*NO1,NO2,NO3,NO4* }.

The fuzzy set of Q_{Ar} is {*PA1,PA2,PA3,PA4* }.

The fuzzy set of W is { *PW1,PW2,PW3,PW4* }.

Fuzzy affiliation function selection triangle function [18,19]. The affiliation functions of variables are shown in Table 1. i, j, m, n, k are the fuzzy partition numbers, which are integer between 1 and 4

Table 1. The affiliation functions of variables

Affiliation functions								
e_1	e_2	e_3	e_4	ec	Q_O	U	Q_{Ar}	W
$\mu(e_{1i})$	$\mu(e_{2i})$	$\mu(e_{3i})$	$\mu(e_{4i})$	$\mu(ec)$	$\mu(Oj)$	$\mu(Um)$	$\mu(An)$	$\mu(Wk)$

2) Fuzzy rule table

The following data are set based on expert experience and production tests. The maximum oxygen supply flow rate during the smelting process is 0.25m^3/s, the maximum height of the top gun is 1.7m, the lowest argon supply flow rate is 0.011m^3/s, the maximum argon supply flow rate is 0.085m^3/s, and the maximum splashing inhibitor is 0.2t. The fuzzy control rules are Table 2 to Table 5.

Table 2. Oxygen supply flow control rules

e / Q_O / ec	e_{11}	e_{12}	e_{13}	e_{14}
P	*NO4*	*NO3*	*NO2*	*NO2*
Z	*NO3*	*NO3*	*NO1*	*NO1*
N	*NO4*	*NO3*	*NO3*	*NO1*

Table 3. Top gun height control rules

e / U / ec	e_{21}	e_{22}	e_{23}	e_{24}
P	*PU1*	*PU1*	*PU2*	*PU2*
Z	*PU2*	*PU2*	*PU3*	*PU3*
N	*PU3*	*PU2*	*PU3*	*PU4*

Table 4. Argon supply flow control rules

e / Q_{Ar} / ec	e_{31}	e_{32}	e_{33}	e_{34}
P	*PA1*	*PA1*	*PA2*	*PA2*
Z	*PA2*	*PA2*	*PA3*	*PA3*
A	*PA3*	*PA2*	*PA3*	*PA4*

Table 5. splashing inhibitor input control rules table

Preprints (www.preprints.org) | NOT PEER-REVIEWED | Posted: 10 June 2022 doi:10.20944/preprints202206.0151.v1

e / W / ec	e_{41}	e_{42}	e_{43}	e_{44}
P	*PW1*	*PW1*	*PW2*	*PW2*
Z	*PW2*	*PW2*	*PW3*	*PW3*
N	*PW3*	*PW2*	*PW3*	*PW4*

3) Fuzzy reasoning and clarity

The fuzzy rules are multi-conditional and the fuzzy relations in matrix form are as follows.

$$R_1 = (e_{11} \times ec \times NO1) \cup (e_{12} \times ec \times NO2) \cup (e_{13} \times ec \times NO3) \cup (e_{14} \times ec \times NO4) \quad (10)$$

$$R_2 = (e_{21} \times ec \times PU1) \cup (e_{22} \times ec \times PU2) \cup (e_{23} \times ec \times PU3) \cup (e_{24} \times ec \times PU4) \quad (11)$$

$$R_3 = (e_{31} \times ec \times PA1) \cup (e_{32} \times ec \times PA2) \cup (e_{33} \times ec \times PA3) \cup (e_{34} \times ec \times PA4) \quad (12)$$

$$R_4 = (e_{41} \times ec \times PW1) \cup (e_{42} \times ec \times PW2) \cup (e_{43} \times ec \times PW3) \cup (e_{44} \times ec \times PW4) \quad (13)$$

According to the splash degree corresponding to the fuzzy rules, the output discrete fuzzy set control quantity is as follows.

$$O_j = T_{1i} \diamond R_1 \quad (14)$$

$$U_m = T_{2i} \diamond R_2 \quad (15)$$

$$A_n = T_{3i} \diamond R_3 \quad (16)$$

$$W_k = T_{4i} \diamond R_4 \quad (17)$$

Where $\diamond$ is the fuzzy decision.

The process of turning a fuzzy quantity into an accurate one is called clarification. In this study, the clarification operation is performed using the weighted average method.

The exact value of the oxygen supply flow rate is shown in the following equation.

$$Q_O = \frac{\sum_{j=1}^{4} O_j \mu(O_j)}{\sum_{j=1}^{4} \mu(O_j)} \quad (18)$$

Where $\mu(O_j)$ is the affiliation function of the oxygen supply flow rate.

The exact value of the top gun height is shown in the following equation.

$$U = \frac{\sum_{m=1}^{4} U_m \mu(U_m)}{\sum_{m=1}^{4} \mu(U_m)} \quad (19)$$

Where $\mu(U_m)$ is the affiliation function of the top gun height.

The exact value of the argon supply flow is shown in the following equation.

$$Q_{Ar} = \frac{\sum_{n=1}^{4} A_n \mu(A_n)}{\sum_{n=1}^{4} \mu(A_n)} \quad (20)$$

Where $\mu(A_n)$ is the affiliation function of the argon supply flow.

The exact value of the splashing inhibitor input is shown in the following equation.

Preprints (www.preprints.org) | NOT PEER-REVIEWED | Posted: 10 June 2022 doi:10.20944/preprints202206.0151.v1

$$W = \frac{\sum_{k=1}^{4} W_k \mu(W_k)}{\sum_{k=1}^{4} \mu(W_k)} \quad (21)$$

Where $\mu(W_k)$ is the affiliation function of the splashing inhibitor.

The above equations are used to calculate the control amount to produce a suppression effect on splashing.

4. Simulation experiment analysis

The control effect is simulated using MATLAB platform. Setting different levels of initial signals, the simulation is analyzed as follows.

The initial signal is set to 0.2. The R_1 rule is adopted to suppress splashing. The simulation curve is shown in Figure 8. As seen from the simulation results, the signal returns to the normal range after 80s. The control system rise time is about 60s, and the steady-state error is 0.

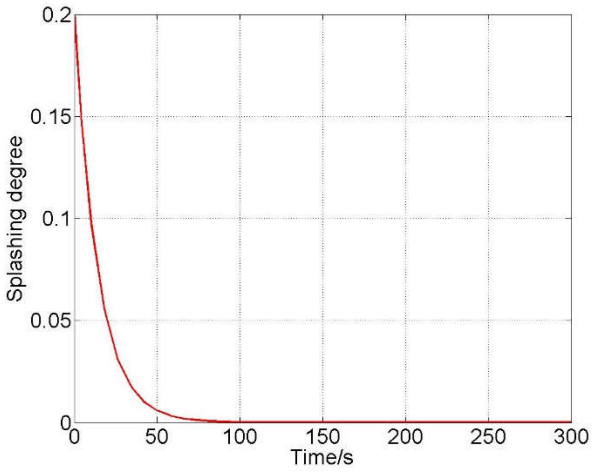

Figure 8. Simulation curve of 0.2 intensity suppression splashing

The initial signal is set to 0.4. The R_2 rule is adopted to suppress splashing. The simulation curve is shown in Figure 9. As seen from the simulation results, the signal returns to the normal range after 100s. The control system rise time is about 80s, and the steady-state error is 0.

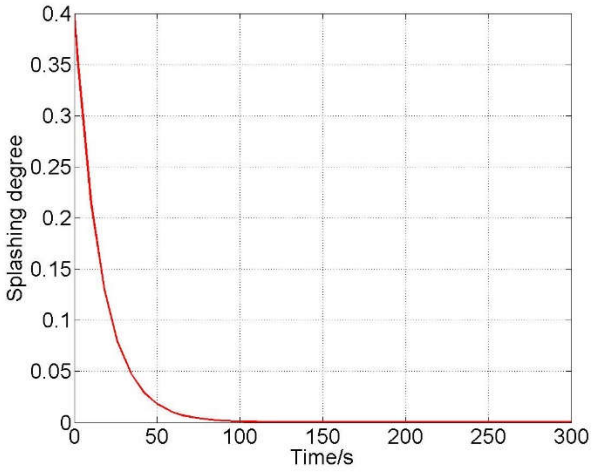

Figure 9. Simulation curve of 0.4 intensity suppression splashing

Preprints (www.preprints.org) | NOT PEER-REVIEWED | Posted: 10 June 2022 doi:10.20944/preprints202206.0151.v1

The initial signal is set to 0.6. The R_3 rule is adopted to suppress splashing. The simulation curve is shown in Figure 10. As seen from the simulation results, the signal returns to the normal range after 130s. The control system rise time is about 110s, and the steady-state error is 0.

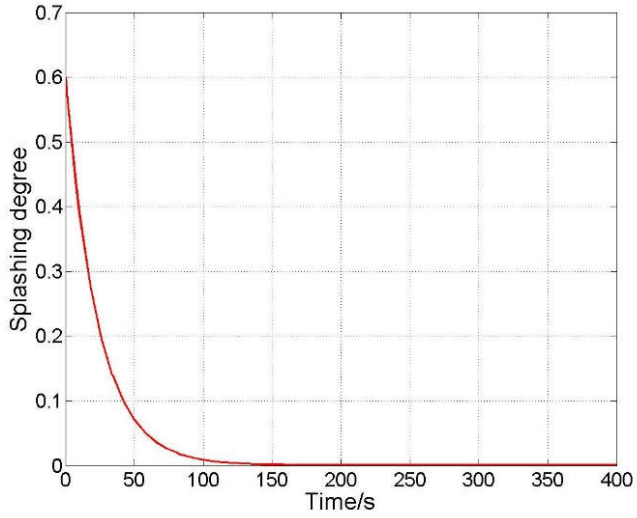

Figure 10. Simulation curve of 0.6 intensity suppression splashing

The initial signal is set to 0.8. The R_4 rule is adopted to suppress splashing. The simulation curve is shown in Figure 11. As seen from the simulation results, the signal returns to the normal range after 180s. The control system rise time is about 150s, and the steady-state error is 0.

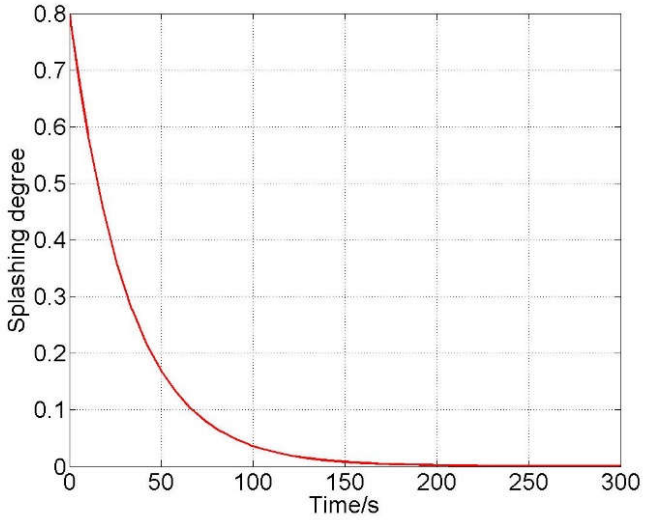

Figure 11. Simulation curve of 0.8 intensity suppression splashing

The above simulation results show that splashing can be quickly suppressed by fuzzy control. The stronger the splashing, the longer the suppression time required.

Preprints (www.preprints.org) | NOT PEER-REVIEWED | Posted: 10 June 2022 doi:10.20944/preprints202206.0151.v1

5. Production trials

Twenty production trials were conducted to verify prediction and suppression splashing effects. The weight, temperature, and melt composition of the initial melt are recorded in Table 6. The C content was between 7.48 to 8.57 wt%, the S_i content was between 1.79 to 2.03 wt%, the Cr content was between 58.70 to 63.36 wt%, and the initial temperature was between 1335 to 1424°C. The data shows that the smelting raw materials used in this work became very stable. It has analytical significance.

Table 6. Initial data of melt

No.	Initial content (wt%)			Initial weight (t)	Initial temperature (℃)	End point temperature (℃)
	C	Cr	S_i			
1#	8.45	62.87	1.80	5.13	1335	1758
2#	8.40	61.58	1.82	5.24	1375	1759
3#	8.31	60.72	1.79	4.75	1343	1749
4#	8.56	62.52	1.89	5.00	1424	1763
5#	8.35	61.97	1.85	4.55	1363	1762
6#	8.57	62.03	1.96	5.28	1368	1765
7#	7.98	61.88	1.81	3.54	1374	1756
8#	8.04	61.48	1.99	5.30	1358	1761
9#	7.81	63.36	1.85	3.18	1378	1756
10#	8.14	60.59	2.01	4.98	1366	1764
11#	8.34	61.33	1.86	5.04	1368	1760
12#	8.20	61.50	2.03	5.34	1347	1764
13#	8.06	62.05	1.88	4.63	1361	1767
14#	7.86	60.84	1.94	4.13	1369	1765
15#	8.42	61.10	2.01	3.89	1378	1767
16#	7.48	58.70	1.79	5.21	1384	1763
17#	8.11	61.87	1.82	4.37	1360	1755
18#	8.20	61.59	1.89	4.62	1371	1764
19#	8.33	60.93	1.85	4.81	1362	1765
20#	7.88	61.47	1.96	4.46	1377	1756

In the Table 7, 6 out of 20 production trials were forecast. The average smelting time with splashing is 180s longer than the average smelting time without splashing. The data shows that the occurrence of splashing and suppression prolonged the smelting time, but after a relatively short period of time it returned to the normal smelting state, and the rate of the severe splashing accidents was 0%.

Preprints (www.preprints.org) | NOT PEER-REVIEWED | Posted: 10 June 2022 doi:10.20944/preprints202206.0151.v1

Table 7. Smelting endpoint data

No.	End point content (wt%)			Smelting time (s)	Splashing moment (s)	Suppression rule
	C (wt%)	Cr (wt%)	S_i (wt%)			
1#	0.45	58.61	0.08	3702	167	R_3
2#	0.48	60.18	0.16	3727	722	R4
3#	0.45	58.03	0.18	3444	No	
4#	0.43	60.09	0.11	3600	No	
5#	0.51	60.62	0.12	3540	No	
6#	0.48	59.71	0.12	3505	No	
7#	0.49	60.26	0.15	3320	No	
8#	0.47	57.87	0.14	3683	528	R3
9#	0.51	60.90	0.15	3425	No	
10#	0.49	58.43	0.11	3580	No	
11#	0.52	58.86	0.10	3543	No	
12#	0.55	57.81	0.17	3653	456	R3
13#	0.51	59.53	0.14	3498	No	
14#	0.47	56.90	0.10	3454	No	
15#	0.52	57.04	0.16	3624	124	R2
16#	0.46	56.63	0.11	3546	No	
17#	0.49	58.77	0.13	3581	No	
18#	0.51	59.25	0.18	3527	No	
19#	0.48	57.52	0.09	3360	No	
20#	0.47	57.81	0.14	3658	589	R4

6. Conclusion

Based on the principle of splashing generation, a prediction splashing method based on multi-information weighted fusion is designed, and a multi-object fuzzy control system is established to suppress splashing. The simulation results indicated that splashing of different degrees can be effectively suppressed within 200 s, and the steady-state error of the system response is 0. This indicates that the control system has a fast response and high steady-state accuracy. The production data analysis indicated that the multi-object fuzzy controller has a good effect of suppressing the system splashing.

Author Contributions: Changjun Guan: Conceptualization, Investigation, Writing – original draft, editing, Supervision & review, Funding acquisition.

Funding: This research was funded by the National Natural Science Foundation of

China (51374040), and the Science Research Foundation of Education Department of Jilin Province (No. JJKH20210740KJ).

Institutional Review Board Statement: Not applicable.

Informed Consent Statement: Not applicable.

Data Availability Statement: Available on request from the corresponding author.

Conflicts of Interest: The authors declare that they have no known competing financial interests or personal relationships that could have appeared to influence the work reported in this paper.

References

1. Liu Y, Ersson M, Liu H, et al. A Review of Physical and Numerical Approaches for the Study of Gas Stirring in Ladle Metallurgy. Metallurgical and Materials Transactions B: Process Metallurgy and Materials Processing Science. 2019;50(1):555-577.
2. Guan CJ, You W. A nonlinear prediction model, incorporating mass transfer theory and expert rules, for refining low-carbon ferrochrome. Journal of the Southern African Institute of Mining and Metallurgy. 2020;120(12):671-680.
3. Brämming M, Björkman B. Avoiding Sloppy BOS Process Behavior. Iron & Steel Technology. 2010;7(11):66-75.
4. Mao JY，You W. Splash prediction method based on AOD furnace flame image feature. Metallurgical Industry Automation. 2020;44(03):36-41+79.
5. Lingyan D, Adams Thomas A. Comparison of steel manufacturing off-gas utilization methods via life cycle analysis. Journal of Cleaner Production. 2020;277,123568.
6. Ji XL，Zhang D. Development and application of high efficiency and intelligent converter smelting technology. Hebei metallurgy. 2020(S1);65-67.
7. Fabritius T M J, Kurkinen P T, Mure P T, et al. Vibration of argon-oxygen decarburisation vessel during gas injection. Ironmaking & Steelmaking. 2005;32(2):113-119.
8. Yenus J, Brooks G, Dunn M, et al. Application of vibration and sound signals in monitoring iron and steelmaking processes. Ironmaking & Steelmaking. 2020;47(2):178-187.
9. Visuri VV, Järvinen M, Kärnä A, et al. A Mathematical Model for Reactions During Top-Blowing in the AOD Process: Validation and Results. Metallurgical and materials transactions B. 2017;48B:1850-1867.
10. Rocchi A, Santecchia E, Ciciulla F, et al. Characterization and Optimization of Level Measurement by an Ultrasonic Sensor System *IEEE Sensors Journal*. 2019;19(8):3077-3084.
11. Francisco J T. A strict formulation of a nonlinear Helmholtz equation for the propagation of sound in bubbly liquids. Part II: Application to ultrasonic cavitation. Ultrasonics Sonochemistry. 2020; 65,105056.
12. Guan CJ, You W. Optimal System for Improved Internal Model Control of Argon Oxygen Decarburization Process Based on Piecewise Linear Model and Time Constant of Filter Optimization. Mathematical Problems in Engineering. 2022;2022(1):1-11.

 doi:10.20944/preprints202206.0151.v1

13. Yu JJ, Hu YP, Wu CM, et al. Palymskiy, Direct numerical simulations of Rayleigh-Bénard convection of a gas-liquid medium near its density maximum. Applied Thermal Engineering. 2020;175,115387.
14. Zhang Z, Raghuvanshi N, Snyder J, et al. Ambient sound propagation. ACM Transactions on Graphics. 2018; 37(6):1-10.
15. Strasberg M. Gas bubbles as sources of sound in liquids. The Journal of the Acoustical Society of America. 1956;28(1):20-26.
16. Richard M, Guillaume R, Frédéric R. Sound generation on bubble coalescence following detachment. International Journal of Multiphase Flow. 2008;34(10):938-949.
17. O'Leary K E, Mucciardi F. The accelerometer as a BOF process control sensor. Steelmaking Conference Proceedings. 1987;70:33-39.
18. Vassilyev S N, Kudinov Y I, Pashchenko F F, et al. Intelligent Control Systems and Fuzzy Controllers. II. Trained Fuzzy Controllers, Fuzzy PID Controllers. Autom Remote Control. 2020;81(5):922-934.
19. Sakthivel R, Selvaraj P, Kaviarasan B. Modified Repetitive Control Design for Nonlinear Systems with Time Delay Based on T-S Fuzzy Model. IEEE Transactions on Systems, Man, and Cybernetics: Systems. 2017;50(2):646-655.